Accepted Manuscript

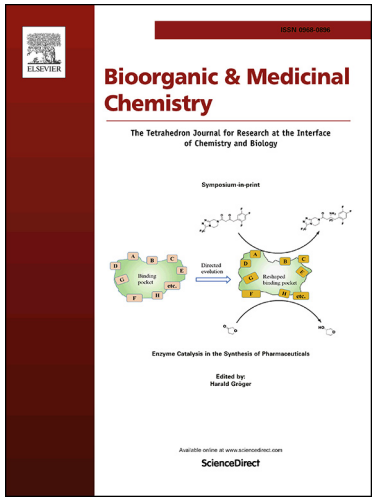

Melanogenic inhibitory effects of Triangularin in B16F0 melanoma cells, *in vitro* and molecular docking studies

María D. Santi, Mariana A. Peralta, Marcelo Puiatti, José Luis Cabrera, María G. Ortega

PII: S0968-0896(19)30390-6
DOI: https://doi.org/10.1016/j.bmc.2019.06.041
Reference: BMC 14978

To appear in: *Bioorganic & Medicinal Chemistry*

Received Date: 8 March 2019
Revised Date: 4 June 2019
Accepted Date: 26 June 2019

Please cite this article as: Santi, M.D., Peralta, M.A., Puiatti, M., Cabrera, J.L., Ortega, M.G., Melanogenic inhibitory effects of Triangularin in B16F0 melanoma cells, *in vitro* and molecular docking studies, *Bioorganic & Medicinal Chemistry* (2019), doi: https://doi.org/10.1016/j.bmc.2019.06.041

Melanogenic inhibitory effects of Triangularin in B16F0 melanoma cells, *in vitro* and molecular docking studies

María D. Santi [a,b], Mariana A. Peralta [a,b], Marcelo Puiatti [c], José Luis Cabrera [a,b], and María G. Ortega [a,b]*

[a] *Farmacognosia, Departamento de Ciencias Farmacéuticas, Facultad de Ciencias Químicas, Universidad Nacional de Córdoba, Ciudad Universitaria, Haya de la torre y Medina Allende, Edificio Ciencias II, X5000HUA Córdoba, Argentina;*

[b] *Instituto Multidisciplinario de Biología Vegetal (IMBIV-CONICET), Ciudad Universitaria. X5000HUA Córdoba, Argentina.*

[c] *Instituto de Investigaciones en Físico-Química de Córdoba (INFIQC), Departamento de Química Orgánica, Facultad de Ciencias Químicas, Universidad Nacional de Córdoba, Ciudad Universitaria, Haya de la torre y Medina Allende, Edificio Ciencias II, X5000HUA Córdoba, Argentina.*

**Corresponding author*

E-mail address: gortega@fcq.unc.edu.ar **(MG Ortega)**

ABSTRACT

The lack of secure therapies for hyperpigmentation disorders, without serious adverse effects, and the latest reports relating melanogenic disorders with development of neurodegenerative diseases, encourage the continuing search for new drugs for the treatment of such disorders. In this sense, the plant kingdom is an important source of bioactive natural products with great potential for the research and development of new therapeutics. The present study evaluated the anti-melanogenic activity of the natural methoxylated chalcone, 2',6'-dihydroxy-4'-methoxy-3'-methylchalcone (Triangularin, **T**), on diphenolase activity from mushroom tyrosinase and on murine B16F0 melanoma cell model. In addition, molecular modelling studies were carried out in order to understand the inhibitory activity observed. **T** showed a potent anti-melanogenic activity being more active than kojic acid (KA) on tyrosinase isolated of both sources and on intracellular tyrosinase. Molecular docking studies displayed important interactions between **T** and the active site of tyrosinase. Our results suggest that **T** may be useful for the treatment of hyperpigmentary disorders.

Abbreviations: T, triangularin; MTT, (3-(4,5-Dimethylthiazol-2-yl)-2,5-diphenyltetrazolium bromide); MNCC, Maximum non-cytotoxic concentration; MBTH, 3-methyl-2-benzothiazolinone; PMSF, Fluorinated phenylmethanesulfonyl; IAA, Iodoacetamide; L-DOPA, L-3,4-dihydroxyphenylalanine; PDB, Protein data bank; 8PP, 4'-dihydroxy-5′-(1‴,1‴-dimethylallyl)-8-prenylpinocembrin; Abs, absorbance; DMEM, Dulbecco's Modified Eagle's medium; FBS ,fetal bovine serum; DMSO, Dimethyl sulfoxide; PBS, Phosphate-buffered saline; KA, kojic acid; SD, standard deviation; IC_{50}, half maximal inhibitory concentration; ANOVA, Analysis of variance.

Keywords: *Dalea elegans*, triangularin, anti-melanogenic activity, molecular modelling studies

1. Introduction

Melanin is the major component of skin color and plays an important role in the prevention of ultraviolet-induced and oxidative stress-induced skin damage. However, excessive accumulation of melanin in the skin surface results in mottled skin; being unfavorable to aesthetics and health conditions.[1–6] Melanogenesis control is the main approach for the treatment of abnormal skin pigmentation disorders.[3,5,7,8]

Tyrosinase is a key enzyme in the melanogenic pathway, responsible for catalyzing two reactions in melanin biosynthesis. First, the hydroxylation of L-tyrosine to L-3,4-dihydroxyphenylalanine (L-DOPA), known as monophenolase enzymatic activity, and further the oxidation of L-DOPA to the corresponding DOPA-dopaquinone, known as diphenolase activity.[3,5,9,10] Therefore, tyrosinase inhibitors are clinically useful for the treatment of dermatological disorders like senile lentigo, ephelides (freckles), solar lentigo (age spots), postinflammatory melanoderma and melasma, and also they are important in the cosmetics industry for whitening and depigmentation after sunburn.[4,5,11] Kojic acid (KA) is one of the most popular depigmentation agents, however, several adverse effects have been reported as genotoxic, hepatocarcinogenic and produce allergic dermatitis.[12] Meanwhile, another depigmentation agent clinically used hydroquinone, causes erythema, stinging, colloid milium, irritation, and allergic contact dermatitis, nail discoloration, paradoxical postinflammatory hypermelanosis. Moreover, its prolonged use led to exogenous ochronosis, permanent discoloration, and permanent leukoderma.[3] Its

clinical use is limited to generating a total depigmentation in patients with diffuse vitiligo.[13]

According to the exposed, the search for new drugs that could be therapeutically useful in the treatment of hyperpigmentary disorders, is necessary and urgent. Therefore, natural sources have become of interest for the search of safe natural compounds with anti-melanogenic activity.[3]

Flavonoids, secondary metabolites obtained from plants, have been reported as important inhibitors of tyrosinase.[14–23]

Our group has studied several species from *Dalea* genus. We had previously reported the isolation, structural elucidation and monophenolase mushroom tyrosinase inhibitory activity of flavonoids from the Argentinean species *Dalea boliviana* Britton[24] and *D. elegans* Gillies ex Hook & Arn.,[25] and from Bolivian species, *D. pazensis* Rusby.[26]

The prenylated flavanone, 4'-dihydroxy-5′-(1‴,1‴-dimethylallyl)-8-prenylpinocembrin (**8PP**) and the methoxylated chalcone 2',6'-dihydroxy-4'-methoxy-3'-methylchalcone [**Triangularin** (**T**), Fig. 1], obtained from *D. elegans*,[25] showed significant monophenolase inhibitory activities on mushroom tyrosinase.[25] In addition, **8PP** presented inhibitory effects on diphenolase mushroom tyrosinase and on melanogenesis of murine melanoma B16F0 line cells.[26]

The aim of this work was to evaluate the anti-melanogenic activity of **T** on *in vitro* and *ex vivo* models. Furthermore, molecular docking studies were performed in

order to explain the inhibitory effect observed and to propose the interaction mode with the enzyme.

2. Results and discussion

*2.1. Effect of **T** on diphenolase activity of mushroom tyrosinase*

The inhibitory activity of the natural compound **T** (Fig. 1) on diphenolase inhibitory activity at different concentrations (1.5-200 μM) was evaluated by an *in vitro* spectrophotometric assay. The IC_{50} value was estimated using the nonlinear fitting of concentration-response data.

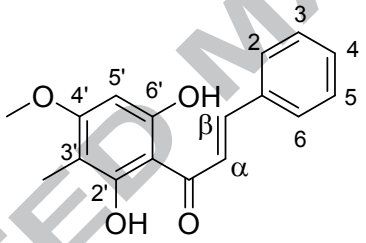

Fig. 1. Structure of 2',6'-dihydroxy-4'-methoxy-3'-methylchalcone (**T**).

T, with an IC_{50} value of (63.1±0.2) μM, was approximately two fold more active than the positive reference, KA [IC_{50}, (129.6±0.3) μM] (Fig. 2). With respect to the study of structure-activity relationship on the tyrosinase inhibitory activity by different chalcones, the presence of the 4-substituted resorcinol moiety in B ring has been demonstrated as a structural requirement necessary to observe inhibitory activity on

tyrosinase. Also, the hydroxylation in 2',4' and 6' positions of A-ring collaborates with this inhibitory activity.[25,27,28] In addition, other studies led to reinforce the relevant presence of the trihydroxyl groups in 2', 4' and 6' positions of A ring for mushroom anti-tyrosinase activity in chalcones. Furthermore, Lall et al., (2016) reported antityrosinase activity of two chalcones: 2',4',6' -trihydroxy-dihydrochalcone and 2',6'-dihydroxy-4'-methoxydihydrochalcone, being the first one active with an IC_{50} of 17.7 µg/ml, and the second completely inactive at 200 µg/ml.[29] Although compound **T** presents a 4'-methoxylated substitution, this compound has an important activity even more than KA. In this sense, the presence of a methyl group in 3' position could be relevant. That observation was then studied by molecular modeling.

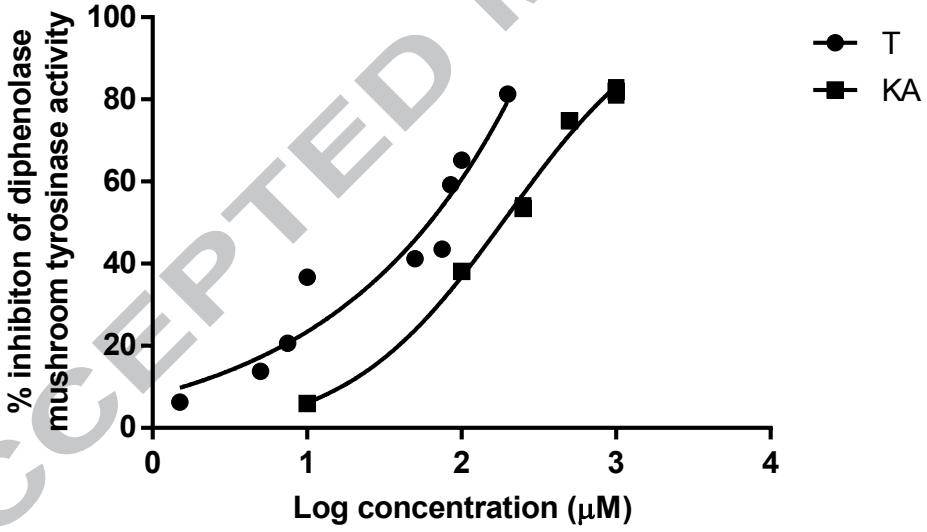

Fig. 2. Dose-dependent inhibition of diphenolase mushroom tyrosinase activity by compound **T** and positive control KA (N = 3).

*2.2. Effect of **T** on tyrosinase isolated from melanoma B16F0 mouse cells activity.*

With the aim of using a model closer to human melanogenesis, the inhibitory activity of **T** at different concentrations (0.001-1000 μM) was compared with that of the reference inhibitor KA (10-5000 μM), being both evaluated against tyrosinase present in crude lysates of B16F0 melanoma cells. A concentration-dependent inhibition was observed. When compound **T** and the reference inhibitor KA effects were compared at 10 μM and 100 μM, **T** proved to be six fold more active than KA at the minimal concentration (Table 1). Then, a concentration-dependent inhibition of melanoma B16F0 murine tyrosinase activity by compound **T** and positive control KA was performed for estimate and compare the IC_{50} values. The Fig. 3 shows the concentration-dependent inhibition curves obtained. **T** proved to be three-fold more active than the reference inhibitor (Table 1).

Table 1. Murine isolated tyrosinase inhibitory activity of compound **T**, and the reference inhibitor, KA.

Compound	Inhibition at 10 μM (%)	Inhibition at 100 μM (%)	IC_{50} (μM)
T	43.74±0.01	61.43±0.01	**30.9±0.3**[a]
KA	7.30±0.02	56.60±0.01	**89.7±0.4**

Mean ± SD of at least 3 determinations. [a]$p < 0.0001$, the IC_{50} value was significantly different from that of KA.

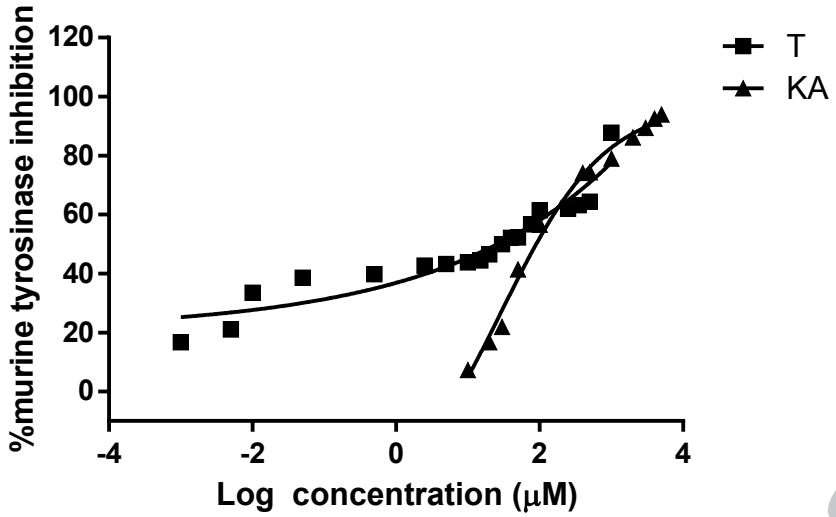

Fig. 3. Concentration-dependent inhibition of melanoma B16F0 murine tyrosinase activity by compound **T** and positive control KA (*N=3*).

In this way, it was observed that **T** showed inhibition on the diphenolase activity of mushroom tyrosinase and on tyrosinase isolated from murine B16F0 melanoma cells, a validated model for melanogenesis study.

2.3. Cell viability assay.

In order to obtain the maximum non-cytotoxic concentration (MNCC, the concentration at which the cells remained at 90% viability) for **T** and KA, the cell viability was determined at different concentrations of the compounds by using MTT spectrophotometric assay as previously described by Santi et al. (2017) [26]. After 24 h of incubation, it was observed that **T** inhibited melanoma B16F0 cells proliferation in a concentration-dependent manner. For **KA**, the value of MNCC was previously

informed by Santi et al. (2017) being (5000±10) μM [26], while for compound **T**, the MNCC estimated showed to be (100.0±2.0) μM. These concentrations were selected to ensure the cell viability, for further experiments developed on melanoma B16F0 cells.

2.4. Effect of Triangularin on extracellular melanin of murine melanoma B16F0 cell line.

With the aim of evaluate the effect of **T** on the production of extracellular melanin on B16F0 cells, without affecting the cell viability, the effect of several concentrations of that compound, below of its MNCC was assayed. The concentration needed to decrease the extracellular melanin content at approximately at 50% was (25.0±0.5) μM for **T**, whereas for the reference inhibitor the required concentration was (2000±5.0) μM.[26] Hence, compound **T** showed to be approximately eighty fold more active than KA (Fig. 4).

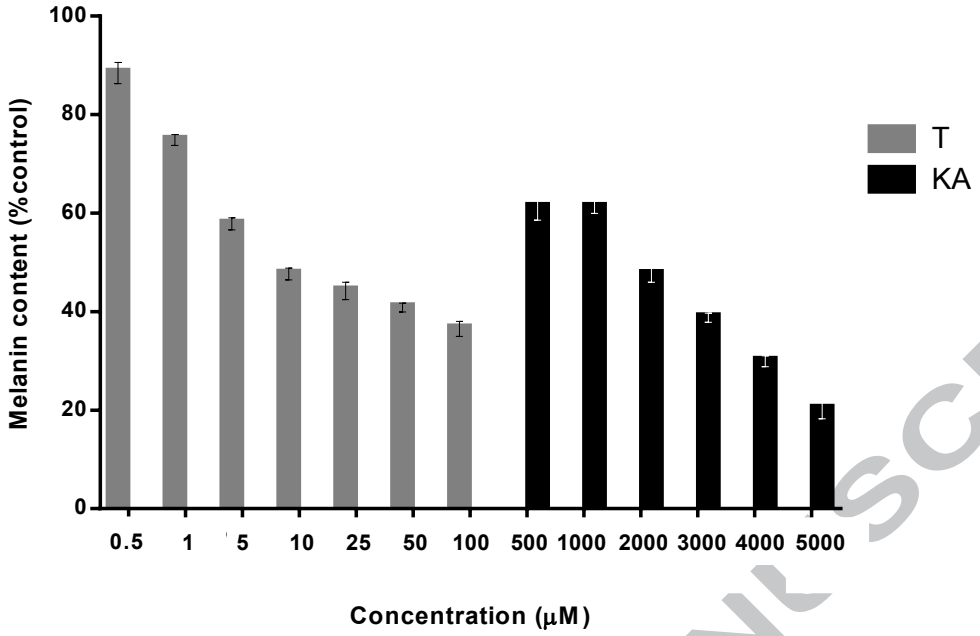

Fig. 4. Melanin content at increasing concentrations of **T** and **KA**. All experimental assays treated with **T** or **KA** were significantly different to the control (without treatment, considered 100% of melanin).

Structure-activity relationship of chalcones on melanogenesis in B16F0 cells have been reported. Chalcones presenting in their structure 4-substitued resorcinol in B ring and three hydroxyl groups in position 2', 4' and 6' of A ring have been reported as inhibitors of the melanogenesis.[30] Additionally, it was reported that the substitution at 3' position of A ring, plays an important role in enhancing the inhibitory activity. Compound **T** presents, in part, these structural characteristics marked as important for the inhibition of melanogenic activity in B16F0 melanoma cells, which could explain the important activity observed for this compound.

According to the obtained results, the influence of **T** on intracellular tyrosinase was evaluated.

2.5. Effect of triangularin on intracellular tyrosinase of murine B16F0 melanoma cells activity.

The B16 cells were incubated for 24 h with different concentrations below of MNCC of **T** or KA and the intracellular tyrosinase activities were evaluated and compared with the control cells. Table 2 shows the intracellular tyrosinase inhibition of **T** and the reference inhibitor, at their MNCC concentration (^{a,b} $p<0.001$, the values are significantly different). The chalcone exerted a concentration-dependent inhibition on intracellular tyrosinase activity (Table 2). At the MNCC, the tyrosinase inhibition achieved for **T** was $(20.1 \pm 0.3)^a$ % at 100 µM, and for the reference inhibitor KA was $(45.4 \pm 0.1)^b$ %, at 5000 µM.[26]

Table 2. Intracellular tyrosinase inhibition for compound **T** and KA at their MNCC.

T concentration (µM)	**% Intracellular tyrosinase inhibition**	**KA concentration (µM)**	**% Intracellular tyrosinase inhibition**
1	(3.9±0.4)	500	$(21.63\pm0.21)^b$
5	(6.1±0.3)	1000	(28.63±0.12)

10	(7.8±0.2)	2000	(37.62±0.2)
25	(12.99±0.3)	3000	(44.62±0.16)
50	(16.23±0.17)	4000	(44.93±0.8)
100	(20.1±0.3)[a]	5000	(45.4±0.1)

Mean ± SD of at least 3 determinations. [a,b]$p > 0.05$, the values are not significantly different statistically

The concentrations of **T** and KA that produced similar inhibitions values were compared. It was observed that **T** inhibits 20.1% at 100 μM, while KA inhibits 21.63% at 500 μM (Table 2). Therefore, compound **T** was more active than KA, showing that are required five fold lower concentrations of **T** compared with the reference inhibitor to generate a similar inhibition.

Although **T** and KA did not show inhibition greater than 50% at their MNCC, the synergism could be a possible pharmacological strategy to be investigated in order to enhance their activities, decreasing the adverse effects of commercial whiteners currently used in clinic.

2.6. Molecular docking studies

With a focus on understand the binding mode of **T** with mushroom tyrosinase trying to explain the origin of its activity, molecular modeling studies were carried out. In the first place, molecular docking calculations were used to build nine different complexes **T** with mushroom tyrosinase. Finally, a short molecular dynamics simulation of each complex followed by an evaluation of the binding

energy were carried out to select the best complex with the enzyme. The obtained binding energies of each complex are included in Table S1 in the supplementary material as well as, figures comparing their geometries (Fig. S1 and S2-ab).

It was found that the more stable complexes presented energies of -27.3 and -26.7 kcal/mol. Even though both complexes could be important, we will only consider the most stable one for the discussion. In Fig. 5, it is a 2-D representation of the binding mode. In insets B, it is shown the RMSD of the ligand during the MD simulation, showing that the geometry of the complex does not vary during the simulation. Analyzing its binding mode, complex 1 included the B ring within the active site interacting with histidines 63 and 85 (coordinated to ones of the Cu atoms of the active site), and with histidines 259 and 263 (Fig. S3). Complex 2 also included the B ring at the active site, with the A ring in the same position as complex 1 (but flipped 180º). Besides these interactions with the B ring, there are other important interactions, an H-bond between the NH of histidine 85 with the oxygen of the hydroxyl group at 2' position and Van der Waals interactions with other residues (Fig. 5, A-D). It was found that the H-bond with H85 persisted during the simulation, and that could be the reason why the interaction with this histidine is the most important one. Additionally, it was observed an important interaction between the 3' methyl and the non-charged polar residue Asn81. That methyl group also presented an interaction with Thr324 residue. These interactions are shown both in the 2D representation of Fig. 5 and in the residue decomposition of the binding energy (Fig. 5 D).

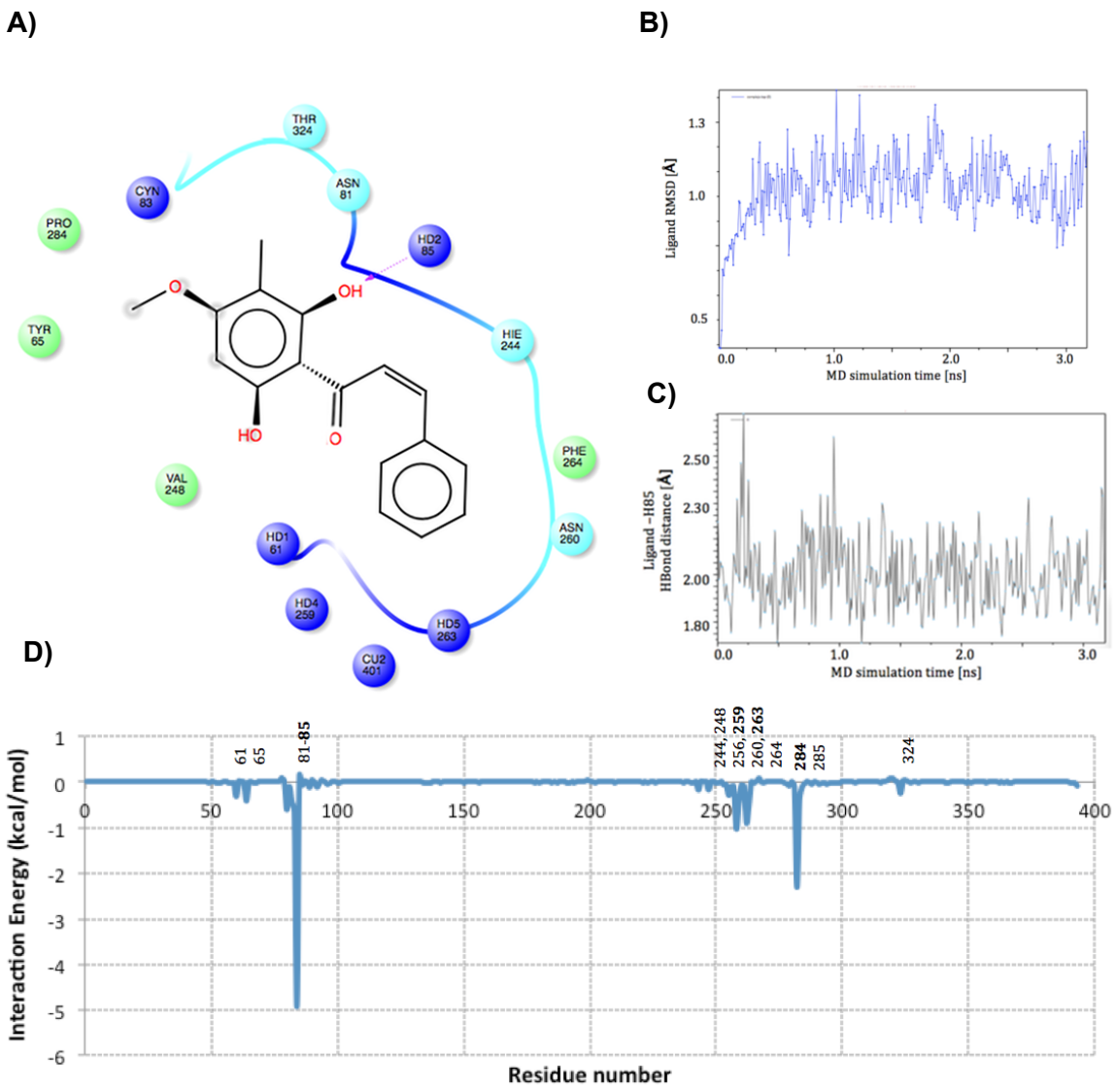

Fig. 5. A) A 2D representation of the best complex between **T** and mushroom tyrosinase showing the interactions of the ligand with the enzyme. In blue, polar interactions with the histidines of the active site, in green, hydrophobic interactions and in light blue polar

interactions. Red arrow indicates an H-Bond. **B)** In the inset it is represented the RMSD of the ligand during the 3ns simulation. **C)** Evolution of the His85 NH-O 2' of the ligand during the simulation. **D)** Graph of interaction energies.

3. Conclusion

In our screening program for tyrosinase inhibitors plant compounds by using mushroom tyrosinase, 2', 6'-dihydroxy-4'-methoxy-3'-methylchalcone (**T**) was isolated and identified from aerial parts of *Dalea elegans.* **T** was previously reported as an inhibitor of monophenolase mushroom tyrosinase activity, and its kinetic mechanism of action was informed.[25] In this work, **T** was evaluated with respect to its diphenolase mushroom tyrosinase activity and its influence on cell viability and melanin synthesis on murine melanoma B16F0 cells, by three *in vitro* assays to screen depigmenting agents. **T** showed to be, in all experimental performed assays, more active than the positive reference KA, thus demonstrating an important anti-melanogenic activity.

The molecular modeling studies showed important interactions between the methoxylated chalcone and catalytic residues of the active site of tyrosinase. The interaction between the 2'-OH and the H85 residue, added to the interaction between 3'-methyl with Asn81 and Thr324 residues could explain at the molecular level, the powerful inhibitory activity observed.

In light of the above, we present, for the first time, a natural chalcone obtained from *D. elegans*, a native Argentinean plant, with demonstrated inhibitory activity of melanogenesis. The present results encourage us to carry out a greater clinical

investigation of Triangularin for hyperpigmentation disorder therapy and in the cosmetic industry.

4. Experimental

4.1. Plant material

D. elegans Gillies ex Hook. et Arn. (Fabaceae) whole plant was collected in February 2012, near Cabalango (Córdoba, Argentina, GPS coordinates: latitude: 31°24'04.62'' South; longitude: 64°34'19.21'' West; height: 763 m). Plant material was identified by Prof. Dr. Gloria Barboza of the Botanical Museum, Universidad Nacional de Córdoba, Córdoba, Argentina (CORD). A representative voucher specimen is on deposit as CORD Peralta 2.

4.2. Chemicals

T (purity 95%) was obtained from *D. elegans* aerial parts and identified as previously described by Peralta et al., (2014).[25]

Tyrosinase (EC 1.14.18.1) from mushroom (3933 U/mg), kojic acid (purity: 99%), L-DOPA (purity: 99%), 3-methyl-2-benzothiazolinone (MBTH, purity: 99%), Fluorinated phenylmethanesulfonyl (PMSF, purity: 99%), Iodoacetamide (IAA, purity: 99%) were obtained from Sigma Chemical Co. (St. Louis, MO, USA).

4.3. Diphenolase mushroom tyrosinase inhibition

Tyrosinase-diphenolase inhibitory activity of **T** was performed by using L-DOPA as a substrate according to Peralta et al., (2014) with slight modification.[25] **T** was dissolved in DMSO (final concentration of 0.1% v/v) and then diluted to different concentrations using DMSO. The reaction media contained 0.25 mL of mushroom tyrosinase solution (200 U/mL), and 0.75 mL of the control solution [Na_3PO_4 buffer (0.1 M, pH 6.8)] or the sample solution of **T**. After incubation at 25 °C for 10 min, 0.50 mL of L-Dopa solution (2.55 mM, Sigma) was added. The absorbance was monitored as dopachrome formation at 475 nm on a Cary Win UV-VIS spectrophotometer, Varian, Inc., Agilent Technologies (Santa Clara, USA). KA was used as a positive control. Each treatment was replicated three times. The percent inhibition of tyrosinase activity was calculated as follows: % inhibition = [($Abs_{control}$ X Abs_{sample})/$Abs_{control}$] X100, where $Abs_{control}$ is the absorbance of the control solution and Abs_{sample} is the absorbance of the sample solution.

4.4. Cell culture

B16F0 murine melanoma cell line was maintained under sterile conditions at 37 °C in a humidified atmosphere of 5% CO_2 in DMEM medium (SIGMA, D6429, St. Louis, MO, USA) supplemented with 10% (v/v) fetal bovine serum (FBS) and 1% streptomycin/ penicillin.

4.5. Diphenolase murine tyrosinase inhibition

B16F0 melanoma cells were lysed with trypsin treatment and centrifuged at 2000 rpm for 10 minutes at 4 °C. The formed pellet was dissolved with cell solubilization buffer (TPisol) [Na_2HPO_4 buffer (10 mM, pH 6.8), 1% Triton, 1% Fluorinated phenylmethanesulfonyl (PMSF), 1% Iodoacetamide (IAA)] and stirred for 40 minutes at 4 °C, and subsequently centrifuged at 14,000 rpm for 30 minutes. A supernatant rich in tyrosinase was obtained, and the protein concentration was determined using the *Bradford* method.[31]

The reaction mixture containing 40 µL of supernatant, 5 µL of **T** or KA dissolved in DMSO (>0.5%), 40 µL of L-DOPA (2.55 mM) and 100 µL of 3-methyl-2-benzothiazolinone (MBTH) was prepared. The absorbance of the MBTH-dopaquinone adduct was followed spectrophotometrically at 490 nm. The % inhibition of intracellular tyrosinase was calculated as the mushroom tyrosinase assay previously described.

4.6. MTT assay

Cell viability was determined as previously described by Santi et al. (2017).[26] Briefly, B16F0 melanoma cells (1 x 10^5) were incubated with 100µl the control solution (fresh media with DMSO 0.5% v/v) or 100 µl of the **T** solution at several concentrations (0.5 to 100 µM) for 24 h. The treatment was replicated for triplicate. After incubation, 100 µl of MTT reagent [3-(4,5-dimethyl-2-thiazolyl)-2,5-diphenyl-2H-tetrazolium bromide in PBS (5 mg/mL)] were added to each well. The plates were incubated in a humidified atmosphere of 5% of CO_2 at 37°C for 30 min. The

residual MTT solutions were removed and then, 100 µl of isopropyl alcohol was added. The absorbance was measured at 595 nm in a microplate reader (*BioTek* ELx800). Then, the MNCC for **T** was determined.

4.7. Measurement of melanin content

The assay was performed as previously described by Santi et al. (2017).[26] Briefly, B16F0 cells were incubated in 24-well plate at a density of 1 10^5 cells per well overnight. The cells were treated with different concentrations of **T** (0.5-100 µM) for 24 h. After that, the extracellular melanin content was calculated relative to the control (without treatment, considered as 100% of the production of melanin) measured at 510 nm using a microplate reader (BioTek ELx800).

4.8. Intracellular tyrosinase inhibition assay

Tyrosinase enzyme activity was assayed spectrophotometrically according to a published method by measuring the formation of the adduct between 3-methyl-2-benzothiazolinone (MBTH) and dopaquinone.[26] Briefly, the reaction mixture composed of cell lysates of pretreated B16F0 cells with different concentrations of **T** or KA, added of 40 µl of L-DOPA (10 mM) and 100 µL of MBTH (5 mM) was kept for 20 min at 37°C. The absorbance of the MBTH-dopaquinone adduct was followed spectrophotometrically at 490 nm. The % inhibition of intracellular tyrosinase was calculated as the mushroom tyrosinase assay.

4.9. Statistical analyses

All assays were independently performed in triplicate, and results were expressed as media ± SD of six separate experiments. The IC_{50} values were estimated using the *GraphPad Prism* 6 software on a compatible computer.

The results were analyzed by unidirectional analysis of variance (ANOVA) followed by the *Tukey* test for multiple comparisons using *GraphPad InstStat* software.

5.0. Molecular modeling

The complexes between the ligands and mushroom tyrosinase were obtained by molecular docking with the software Autodock VINA.[32] The GPU version of Amber14 was used for carrying out molecular dynamics simulations [33,34] and VMD [35] and Maestro [36] were used for the analysis of results and preparation of figures.

The starting coordinates of the protein were taken from reference, PDB code: 2Y9W.[37] The metal center was parameterized using the tool MCPB.py. [38] Care should be taken when treating copper, since the recommended non-bonded parameters [39] for this metal center did not work properly, and we replaced them by the ones employed by other authors.[40–42] The amberff14SB [43] was employed for the protein residues and the properties of the ligands were obtained by using antechamber [44] with RESP charges.[45] A list with geometries of the ligand is included in the Supplementary Information.

For the docking, two boxes were used (Fig. S4). In a first approximation, a big box of (28.0 × 22.5 × 24.0) Å with a grid spacing of 0.325 Å was used. After these first docking calculations, it was found that the most stable complexes located the inhibitor around the active site, hence a smaller box of (10.0 × 17.0 × 10.0) Å was used to refine the docking search.

After each docking calculation, 9 geometries were obtained and a refinement and recalculation of the binding energy were carried out for each complex to select the best of each ligand. The refinement consisted of two 5,000 steps of minimization, one with restrictions in the movement of protein atoms, and the other with restrictions in only the residues of the active site (histidines 61, 85, 94, 259, 263 and 296, cysteine 83 and the cooper center) and the ligand. After the minimization, the system was solvated with TIP3P water forming an octahedral box, and then 4 ns of molecular simulations were carried out at 300 K, with only one restriction, the position of the atoms of the Cu center. The simulations were carried out within the PME approximation, implemented in the GPU version of Amber14.[33,34] An average of the binding energy was calculated by selecting 50 snapshots of the last ns of each simulation by using MMPBSA.py tool within a Generalized Born solvation model.[46]

Declaration of interest: none.

Acknowledges

This work was supported by ANPCyT BIDePICT 1576, CONICET D32/10, SECYT-Universidad Nacional de Cordoba (05/C375), MINCyT Cba PID 2010. M.D.S. is postdoctoral fellows of CONICET. M.A.P, M.P., J.L.C. and M.G.O. are members of the Research Career of CONICET. All calculations were performed with computational resources from the Centro de Computación de Alto Desempeño - Universidad Nacional de Córdoba (http://ccad.unc.edu.ar/), in particular the Mendieta Cluster that belongs to the Facultad de Matemática, Astronomía y Física, that is also part of SNCAD - MinCyT, República Argentina. We are indebted to Dr. Brenda Konigheim for her assistance with cells experiments.

References

1. Yamauchi K, Mitsunaga T, Itakura Y, Batubara I. Extracellular melanogenesis inhibitory activity and the structure-activity relationships of ugonins from Helminthostachys zeylanica roots. *Fitoterapia*. 2015;104:69-74. doi:10.1016/j.fitote.2015.05.006
2. Sassi A, Maatouk M, El gueder D, et al. Chrysin, a natural and biologically active flavonoid suppresses tumor growth of mouse B16F10 melanoma cells: In vitro and in vivo study. *Chem Biol Interact*. 2018;283(June 2017):10-19. doi:10.1016/j.cbi.2017.11.022
3. Chatatikun M, Yamauchi T, Yamasaki K, Aiba S. Anti melanogenic effect of Croton roxburghii and Croton sublyratus leaves in a -MSH stimulated B16F10 cells. *J Tradit Chinese Med Sci*. 2018:1-7. doi:10.1016/j.jtcme.2017.12.002
4. Jin Q, Han XH, Yun CY, et al. Melanogenesis inhibitory pregnane glycosides from Cynanchum atratum. *Bioorganic Med Chem Lett*. 2018;28(7):1252-1256. doi:10.1016/j.bmcl.2018.01.004
5. Cho YH, Park JE, Lim DS, Lee JS. Tranexamic acid inhibits melanogenesis by

activating the autophagy system in cultured melanoma cells. *J Dermatol Sci*. 2017;88(1):96-102. doi:10.1016/j.jdermsci.2017.05.019

6. Shin JS, Cho JH, Lee H, et al. Dual hypopigmentary effects of punicalagin via the ERK and Akt pathways. *Biomed Pharmacother*. 2017;92:122-127. doi:10.1016/j.biopha.2017.05.070
7. Nasr Bouzaiene N, Chaabane F, Sassi A, Chekir-Ghedira L, Ghedira K. Effect of apigenin-7-glucoside, genkwanin and naringenin on tyrosinase activity and melanin synthesis in B16F10 melanoma cells. *Life Sci*. 2016;144:80-85. doi:10.1016/j.lfs.2015.11.030
8. Sim MO, Ham JR, Lee MK. Young leaves of reed (Phragmites communis) suppress melanogenesis and oxidative stress in B16F10 melanoma cells. *Biomed Pharmacother*. 2017;93:165-171. doi:10.1016/j.biopha.2017.06.037
9. Jiang R, Xu XH, Wang K, et al. Ethyl acetate extract from Panax ginseng C.A. Meyer and its main constituents inhibit α-melanocyte-stimulating hormone-induced melanogenesis by suppressing oxidative stress in B16 mouse melanoma cells. *J Ethnopharmacol*. 2017;208(15):149-156. doi:10.1016/j.jep.2017.07.004
10. Pillaiyar T, Manickam M, Jung SH. Recent development of signaling pathways inhibitors of melanogenesis. *Cell Signal*. 2017;40(September):99-115. doi:10.1016/j.cellsig.2017.09.004
11. Radhakrishnan S, Shimmon R, Conn C, Baker A. Design, synthesis and biological evaluation of hydroxy substituted amino chalcone compounds for antityrosinase activity in B16 cells. *Bioorg Chem*. 2015;62:117-123. doi:10.1016/j.bioorg.2015.08.005
12. Seo SY, Sharma VK, Sharma N. Mushroom tyrosinase: Recent prospects. *J Agric Food Chem*. 2003;51(10):2837-2853. doi:10.1021/jf020826f
13. Njoo MD, Westerhof W, Bos JD, Bossuyt PMM. The development of guidelines for the treatment of vitiligo. *Arch Dermatol*. 1999;135(12):1514-1521.
http://ovidsp.ovid.com/ovidweb.cgi?T=JS&PAGE=reference&D=emed4&NEW

S=N&AN=1999431950.

14. Kubo I, Kinst-Hori I, Chaudhuri SK, Kubo Y, Sánchez Y, Ogura T. Flavonols from Heterotheca inuloides: Tyrosinase inhibitory activity and structural criteria. *Bioorganic Med Chem*. 2000;8(7):1749-1755. doi:10.1016/S0968-0896(00)00102-4
15. Lee NK, Son KH, Chang HW, Kang SS, Park H, Heo MY. Prenylated Flavonoids as Tyrosinase Inhibitors. *Arch Pharm Res*. 2004;27(11):1132-1135. doi:10.1007/BF02975118
16. Solano F, Briganti S, Picardo M, Ghanem G. Hypopigmenting agents: An updated review on biological, chemical and clinical aspects. *Pigment Cell Res*. 2006;19(6):550-571. doi:10.1111/j.1600-0749.2006.00334.x
17. Karioti A, Protopappa A, Megoulas N, Skaltsa H. Identification of tyrosinase inhibitors from Marrubium velutinum and Marrubium cylleneum. *Bioorganic Med Chem*. 2007;15(7):2708-2714. doi:10.1016/j.bmc.2007.01.035
18. Gao H, Nishida J, Saito S, Kawabata J. Inhibitory effects of 5,6,7-trihydroxyflavones on tyrosinase. *Molecules*. 2007;12(1):86-97. doi:10.3390/12010086
19. Saewan N, Koysomboon S, Chantrapromma K. Anti-tyrosinase and anti-cancer activities of flavonoids from Blumea balsamifera DC. *J Med Plants Res*. 2011;5(6):1018-1025. http://scholar.google.com/scholar?hl=en&btnG=Search&q=intitle:Anti-tyrosinase+and+anti-cancer+activities+of+flavonoids+from+Blumea+balsamifera+DC#0.
20. Si YX, Wang ZJ, Park D, et al. Effect of hesperetin on tyrosinase: Inhibition kinetics integrated computational simulation study. *Int J Biol Macromol*. 2012;50(1):257-262. doi:10.1016/j.ijbiomac.2011.11.001
21. Ko HH, Chiang YC, Tsai MH, et al. Eupafolin, a skin whitening flavonoid isolated from Phyla nodiflora, downregulated melanogenesis: Role of MAPK and Akt pathways. *J Ethnopharmacol*. 2014;151(1):386-393. doi:10.1016/j.jep.2013.10.054

22. Orhan IE, Khan MTH. Flavonoid Derivatives As Potent Tyrosinase Inhibitors – A Survey of Recent Findings Between 2008-2013. *Curr Top Med Chem*. 2014;14:1486-1493. doi:10.2174/1568026614666140523120741
23. Chen C, Lin L, Yang W, Bordon J, Wang HD. An Updated Organic Classification of Tyrosinase Inhibitors on Melanin Biosynthesis. 2015:4-18.
24. Peralta MA, Ortega MG, Agnese AM, Cabrera JL. Prenylated flavanones with anti-tyrosinase activity from Dalea boliviana. *J Nat Prod*. 2011;74(2):158-162. doi:10.1021/np1004664
25. Peralta MA, Santi MD, Agnese AM, Cabrera JL, Ortega MG. Flavanoids from Dalea elegans: Chemical reassignment and determination of kinetics parameters related to their anti-tyrosinase activity. *Phytochem Lett*. 2014;10:260-267. doi:10.1016/j.phytol.2014.10.012
26. Santi MD, Peralta MA, Mendoza CS, Cabrera JL, Ortega MG. Chemical and bioactivity of flavanones obtained from roots of Dalea pazensis Rusby. *Bioorganic Med Chem Lett*. 2017;27(8):1789-1794. doi:10.1016/j.bmcl.2017.02.058
27. Jun N, Hong G, Jun K. Synthesis and evaluation of 2′,4′,6′-trihydroxychalcones as a new class of tyrosinase inhibitors. *Bioorganic Med Chem*. 2007;15(6):2396-2402. doi:10.1016/j.bmc.2007.01.017
28. Chang TS. An updated review of tyrosinase inhibitors. *Int J Mol Sci*. 2009;10(6):2440-2475. doi:10.3390/ijms10062440
29. Lall N, Mogapi E, de Canha MN, et al. Insights into tyrosinase inhibition by compounds isolated from Greyia radlkoferi Szyszyl using biological activity, molecular docking and gene expression analysis. *Bioorganic Med Chem*. 2016;24(22):5953-5959. doi:10.1016/j.bmc.2016.09.054
30. Pillaiyar T, Manickam M, Namasivayam V. Skin whitening agents: Medicinal chemistry perspective of tyrosinase inhibitors. *J Enzyme Inhib Med Chem*. 2017;32(1):403-425. doi:10.1080/14756366.2016.1256882
31. Bradford MM. A rapid and sensitive method for the quantitation of microgram quantities of protein utilizing the principle of protein-dye binding. *Anal*

Biochem. 1976;72:248-254.

32. Trott, O., Olson AJ. AutoDock Vina: improving the speed and accuracy of docking with a new scoring function, efficient optimization and multithreading. *J Comput Chem*. 2010;31:455-461. doi:doi:10.1002/jcc.21334.
33. Salomon-Ferrer R, Goetz AW, Poole D, Le Grand S, Walker RC. Routine microsecond molecular dynamics simulations with AMBER - Part II: Particle mesh Ewald. *J Chem Theory Comput*. 2013;9:3878-3888.
34. Le Grand S, Goetz AW, Walker R. SPFP: Speed without compromise - a mixed precision model for GPU accelerated molecular dynamics simulations. *Comp Phys Comm*. 2013;184:374-380.
35. Humphrey W, Dalke A, Schulten K. VMD - Visual Molecular Dynamics. *J Molec Graph*. 14:33-38.
36. Maestro Version 10.6.014 MmV 3. 4. 01. Release 2016-2, Platform Darwin-x86_64. 2016. Maestro, Schrödinger, LLC, New York, NY.
37. Ismaya WT, Rozeboom HJ, Weijn A, et al. Crystal structure of Agaricus bisporus mushroom tyrosinase: identity of the tetramer subunits and interaction with tropolone. *Biochem*. 2011;50:5477-5486.
38. Li P, Merz Jr. KM. MCPB.py: a python based Metal Center Parameter Builder. *J Chem Inf Model*. 2016;56:599-604.
39. Li P, Song LF, Jr. MKM. Systematic parameterization of monovalent ions employing the nonbonded model. *J Chem Theory Comput*. 2015;11:1645-1657.
40. Lucas MF, Monza E, Jorgensen LJ, et al. Simulating substrate recognition and oxidation in laccases: from description to design. *J Chem Theory Comput*. 2017;13:1462-1467.
41. Acebes S, Fernandez-Fueyo E, Monza E, et al. Rational enzyme engineering through biophysical and biochemical modeling. *ACS Catal*. 2016;6:1624-1629.
42. Deri B, Kanteev M, Goldfeder M, et al. The unravelling of the complex pattern of tyrosinase inhibition. *Sci Rep*. 2016;(6):34993.
43. Maier JA, Martinez C, Kasavajhala K, Wickstrom L, Hauser KE, Simmerling C.

Ff14sb: Improving the accuracy of protein side chain and backbone parameters from Ff99sb. *J Chem Theory Comput*. 2015;11:3696-3713.

44. Wang J, Wang W, Kollman PA, Case DA. Automatic atom type and bond type perception in molecular mechanical calculations. *J Mol Graph Model*. 2006;25:247-260.
45. Bayly CI, Cieplak P, Cornell W, Kollman PA. A well-Behaved electrostatic potential based method using charge restraints for deriving atomic charges: the resp. model. *J Phys Chem*. 1993;97:10269-10280.
46. Onufriev A, Bashford D, Case DA. Exploring protein native states and large-scale conformational changes with a modified generalized born model. *Proteins*. 2004;55:383-394.

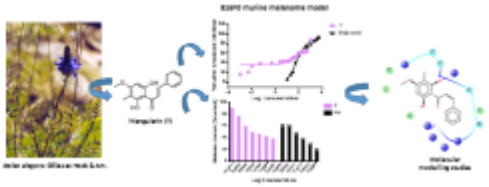

Highlights

- Melanogenic inhibitory activity of a natural methoxylated chalcone was determinate.
- Triangularin was more active than kojic acid in the two models evaluated.
- Docking studies were determined for triangularin for the first time